SIMULATION RESULTS FOR THE ELECTRON-CLOUD AT THE PSR*

M. A. Furman and M. Pivi†, LBNL, Berkeley, CA 94720, USA

Abstract

We present a first set of computer simulations for the main features of the electron cloud at the Proton Storage Ring (PSR), particularly its energy spectrum. We compare our results with recent measurements, which have been obtained by means of dedicated probes.

1 INTRODUCTION

For many years the PSR at Los Alamos has observed a fast instability that is responsible for proton losses and collective beam motion above a certain current threshold, and is accompanied by a large number of electrons. This instability is now believed, though not conclusively proven, to be due to the collective coupling between an electron cloud and the proton beam [1, 2]. Such instability is a particular manifestation of the electron-cloud effect (ECE) that has been observed or is expected at various other machines [3].

In this article we present simulation results for the PSR ring obtained with the ECE code that has been developed at LBNL over the past 5 years, suitably augmented to deal with very long and intense bunches such as in the case of the PSR. At the present stage, we have restricted our studies to look in detail at the dynamics of the electron cloud rather than the instability *per se*. Thus in all results presented here, the proton beam is assumed to be a static distribution of given charge and shape moving on its nominal closed orbit, while the electrons are treated fully dynamically. This approximation is valid for stable beam operation, and it is probably reasonable for mild instability. We defer issues like the current instability threshold, growth rate and frequency spectrum to future studies. We compare our results for the electron current and energy spectrum of the electrons hitting the walls of the chamber against measurements [2] obtained by means of dedicated electron probes [4]. From such comparisons we can assess the effects of several important parameters such as the secondary electron yield (SEY) at the walls of the chamber, the proton loss rate and electron yield, etc. Furthermore, we can infer details of the electron cloud in the vicinity of the proton beam, such as the neutralization factor, which is important for a self-consistent treatment of the coupled e-p problem [5].

2 PHYSICAL MODEL

2.1 Sources of electrons

In this article we consider only what we believe to be the main two sources of electrons, namely: (1) lost protons hitting the vacuum chamber walls, and (2) secondary emission from electrons hitting the walls (we are not interested here in simulating the electron cloud in the vicinity of the stripper foil). Although our code accommodates other sources of electrons, such as residual gas ionization, we have turned them off for the purposes of this article.

We represent the SEY $\delta(E_0)$ and the corresponding emitted-electron energy spectrum $d\delta/dE$ (E_0 =incident electron energy, E = emitted secondary energy) by a detailed model described elsewhere [6, 7]. Its parameters were obtained from detailed fits to the measured SEY and spectrum of stainless steel (St. St.) [8]. The main parameters are the energy E_{max} at which $\delta(E_0)$ is maximum, and the peak value itself, $\delta_{\text{max}} = \delta(E_{\text{max}})$ (see Table 1). However, for most of the results shown below, we *do not* take into account the backscattered and redifused components of $d\delta/dE$. We comment on this fact in Sec. 4.

Table 1: Simulation parameters for the PSR.

Parameter	Symbol	Value
Circumference	C	90 m
Beam energy	E	1.735 GeV
Bunch population	N_p	5×10^{13}
Full bunch length	τ_b	~ 254 ns
Gap length	τ_g	~ 100 ns
Trans. bunch size	$\sigma_x = \sigma_y$	1 cm
Beam pipe radius	a	5 cm
Proton loss rate	p_{loss}	4×10^{-6}
Proton loss yield	Y	100
Beam pipe material		St. St.
SEY params.	$\delta_{\text{max}},\ E_{\text{max}}$	2.05, 300 eV
Number of kicks	N_k	1001
No. of steps in gap	N_g	100

2.2 Simulation Model

The PSR ring stores a single proton bunch of length τ_b followed by a gap of length τ_g with a typical current intensity profile shown in Figs. 1 and 2. In our simulation we assume a Gaussian transverse profile with rms sizes $\sigma_x,\ \sigma_y$, and we use the actually measured longitudinal intensity profile. We simulate the passage of the proton bunch in a field-free section with a vacuum chamber which we take to be a cylindrical perfectly-conducting pipe of radius a. The number of electrons generated by lost protons hitting the vacuum chamber wall is $N_p \times Y \times p_{\text{loss}}$ per turn for the whole ring, where Y is the effective electron yield per lost proton, and p_{loss} is the proton loss rate per turn for the whole ring per beam proton. We assume the lost-

* Work supported by the SNS project and by the US DOE under contract DE-AC03-76SF00098.

† mafurman@lbl.gov and mpivi@lbl.gov

proton time distribution to be proportional to the instantaneous bunch intensity.

The electrons are then simulated by macroparticles. We typically use 1000 macroparticles per bunch passage to represent the electrons generated by the lost protons in the section being simulated. The secondary electron mechanism adds to these a variable number of macroparticles, generated according to the SEY model mentioned above. The bunch is divided up into slices, so that the macroparticles experience N_k kicks during the bunch passage. We divide the interbunch gap into N_g intermediate steps. The space-charge force is computed and applied at each slice in the bunch and each step in the gap. The image forces from both protons and electrons are taken into account, assuming a perfectly conducting wall. Typical parameter values are shown in Table 1.

3 RESULTS

The current and energy distribution of the electrons hitting the vacuum chamber wall have been measured with dedicated probes [2]. A typical measurement is shown in Fig. 1; Fig. 2 shows our simulation result, for which we assume unit detector efficiency and acceptance.

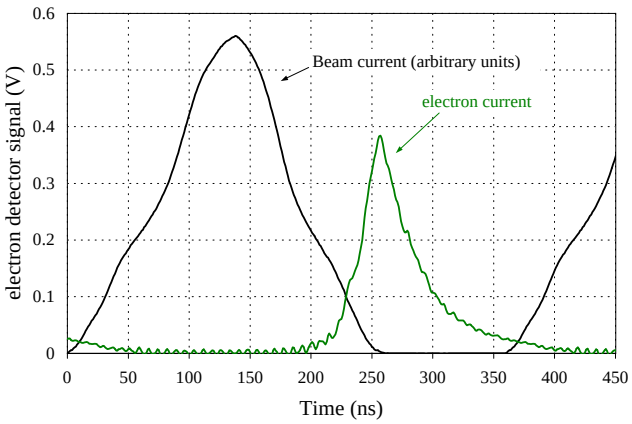

Figure 1: Measured electron detector (ED02X) signal. To obtain the electron current in A/cm^2 one must divide the signal by a factor of 2755.

By applying a negative potential on the second grid of the electron probe it is possible to select the electrons with an energy sufficient to pass the repeller voltage and thus measure their integrated energy distribution. A typical measurement of the cummulative energy spectrum is shown in Fig. 3; our simulation result is shown in Fig. 4.

An important parameter for instability studies is the neutralization factor $\chi \equiv d_e/d_p$, where $d_e(d_p)$ is the local electron(proton) population density. Our result is shown in Fig. 5, indicating that $\chi \gtrsim 0.1$.

4 DISCUSSION AND CONCLUSION

The simulation results are in good qualitative agreement with the experimental data. The peak simulated current of

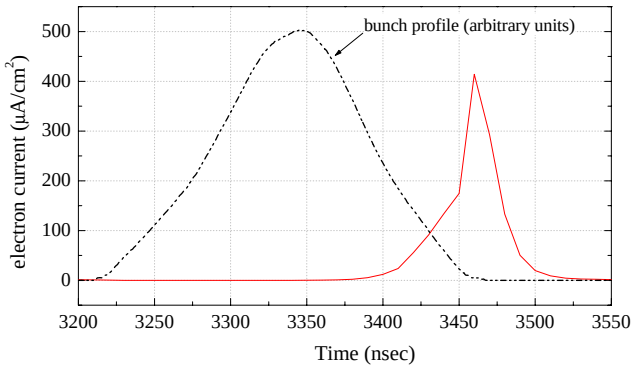

Figure 2: Simulated electron current, assuming unit detector efficiency and acceptance.

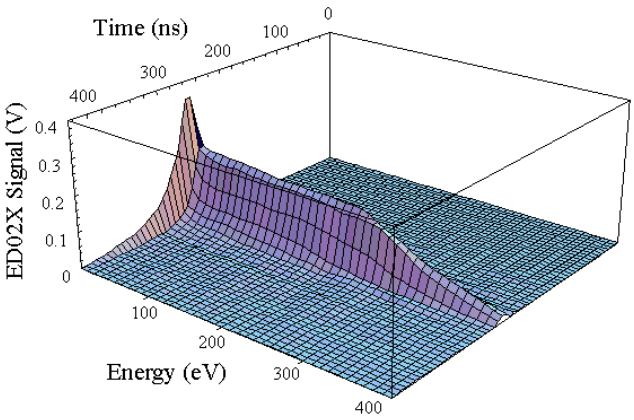

Figure 3: Measured cummulative energy spectrum of the electrons hitting the wall as a function of time (the origin of time does not correspond to the passage of the head of the bunch). To obtain the electron current in A/cm^2 one must divide the voltage signal by a factor of 2755.

$\sim 450\ \mu$A/cm^2 (Fig. 2) agrees better, but not perfectly, with the peak measured value of $\sim 140\ \mu$A/cm^2 (Fig. 1), when the detector efficiency and acceptance are taken into account. The measured peak of the electron distribution at the wall (obtained by differentiating the cummulative spectrum with respect to energy) is at ~ 240 eV is in rough agreement with the corresponding simulated number, ~ 180 eV.

The simulations show that the electrons generated by proton losses are pulled into the beam during the leading edge of the bunch, and are released during the trailing edge. During the trailing edge the average energy of the electrons hitting the wall is $\gtrsim 150$ eV hence the effective SEY is > 1 and the electron cloud intensity increases, corresponding to the so-called "trailing-edge multipacting mechanism" [9]. During the gap the electrons hit the vacuum chamber many times and their average energy decreases hence the effective SEY becomes < 1, thus the walls act as a net absorber of electrons. For typical St. St. SEY parameters, however, the gap between bunches is not long enough to completely clear the electrons. Thus, following injection of the beam into an empty chamber, the electrons gradually increase

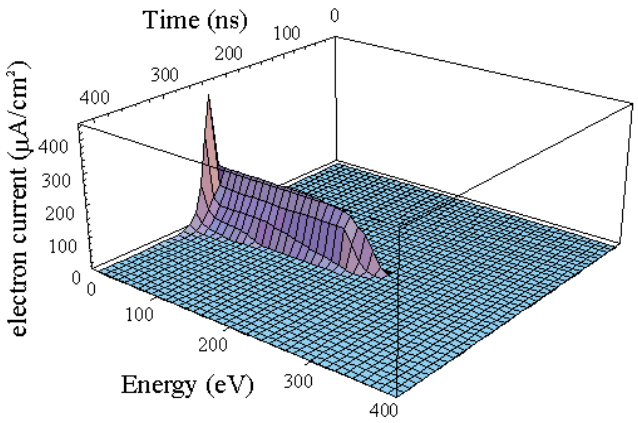

Figure 4: Simulated cummulative energy spectrum of the electrons hitting the wall as a function of time (the origin of time corresponds to the passage of the head of the bunch).

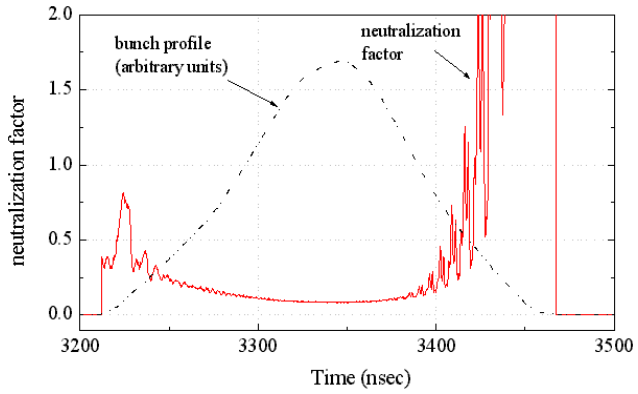

Figure 5: Simulated neutralization factor χ computed within the one-sigma beam ellipse. The growth of χ at both edges of the bunch is dominated by the falloff of d_p.

in number during successive bunch passages until, owing to the space-charge forces, a balance is reached between emitted and absorbed electrons. For our chosen parameter values, this equilibrium is sensibly reached in a few bunch passages.

In the simulation results shown above we truncated the SEY model by neglecting the backscattered and rediffused components of $d\delta/dE$, and took into account only the true secondary component. In addition, we assumed the single-electron emitted-energy spectrum (which is *not* the same as the secondary spectrum $d\delta/dE$) to be Maxwellian in velocity, *i.e.*, of the form $f(E) \propto \sqrt{E}\exp(-E/\epsilon)$ in energy, where $\epsilon = 3.5$ eV. We have investigated the sensitivity of the results to various SEY parameters and we have found a strong and puzzling dependence on the details of $d\delta/dE$, stronger, in fact, than on $\delta_{\rm max}$, for reasonable ranges of values. For example, when we included the rediffused and backscattered components in such a way that $d\delta/dE$ is in good agreement with bench measurements [8], and such that $\delta(0) \simeq 0.1$ and $\delta_{\rm max}$ is kept fixed at 2.05, the simulated peak detector current decreased from ~ 450 to ~ 5 μA/cm^2.

The value of $\delta(E_0)$ at incident electron energies $E_0 \lesssim 10$ eV is an important parameter since it determines the electron accumulation rate, and also the electron survival rate at the end of the gap. This quantity is difficult to measure experimentally and is currently under study at CERN and at SLAC for technical surface materials. We have repeated our simulations under the assumption of $\delta(0) = 0.6$, generally considered to be a high value. In this case, the simulated peak detector current increases by almost a factor ~ 2 relative to the $\delta(0) \simeq 0.1$ case, and the electron density at the end of the gap by a factor ~ 5. These are examples of strong parameter sensitivity that calls for further investigations.

These simulations results represent a first attempt to understand the data, and we have only preliminary information on the sensitivity of the results to various model parameters, most of which are not well pinned down experimentally. We have only considered here the electrons generated by proton losses; residual-gas ionization, possibly compounded by electron-stimulated gas desorption, may lead to significant contributions, and should be simulated.

5 ACKNOWLEDGMENTS

We are grateful to our colleagues of the PSR Instability Studies Program for many discussions. We are especially grateful to R. Macek for discussions and for providing us the data in Figs. 1 and 3. We are indebted to R. Kirby for providing us data on the SEY. We are grateful to NERSC for supercomputer support.

6 REFERENCES

[1] For a summary, see Proc. ICFA Workshop on Two-Stream Instabilities, Santa Fe, NM, Feb. 16–18, 2000, http://www.aps.anl.gov/conferences/icfa/two-stream.html

[2] R. Macek, these proceedings.

[3] G. Rumolo, F. Ruggiero and F. Zimmermann, PRST-AB **4**, 012801 (2001) (erratum: **4**, 029901 (2001)). See also F. Zimmermann, these proceedings.

[4] R. A. Rosenberg and K. C. Harkay, NIMPR **A453** (2000), 507–513.

[5] For an update on the self-consistent treatment of the instability see, for example, the contributions by H. Qin and T. S. Wang, these proceedings.

[6] M. A. Furman and G. R. Lambertson, Proc. Intl. Workshop on Multibunch Instabilities in Future Electron and Positron Accelerators (MBI-97), KEK, Tsukuba, Japan, 15-18 July 1997 (KEK Proceedings 97-17, Dec. 1997, p. 170); http://www.lbl.gov/~miguel/MBI97-ECI-PEPII.pdf

[7] M. A. Furman, LBNL-41482/CBP Note 247/LHC Project Report 180, May 20, 1998, http://www.lbl.gov/~miguel/LHCpr180.pdf

[8] R. Kirby, private communication.

[9] V. Danilov *et al.*, Proc. Workshop on Instabilities of High-Intensity Hadron Beams in Rings, Upton, NY, June 1999 (AIP Conf. Proc. 496, p. 315).